

Behavior of continuous RC deep girders that support walls with long end shear spans

Han-Seon Lee^{1*}, Dong-Woo Ko^{2a} and Sung-Min Sun^{3b}

¹*School of Civil, Environmental, and Architectural Engineering, Korea University, Korea*

²*Department of Architectural Engineering, Jeju National University, Korea*

³*Hyundai Engineering Co. Ltd, Korea*

(Received April 26, 2010, Accepted October 20, 2010)

Abstract. Continuous deep girders which transmit the gravity load from the upper wall to the lower columns have frequently long end shear spans between the boundary of the upper wall and the face of the lower column. This paper presents the results of tests and analyses performed on three 1:2.5 scale specimens with long end shear spans, (the ratios of shear-span/total depth: $1.8 < a/h < 2.5$): one designed by the conventional approach using the beam theory and two by the strut-and-tie approach. The conclusions are as follows: (1) the yielding strength of the continuous RC deep girders is controlled by the tensile yielding of the bottom longitudinal reinforcements, being much larger than the nominal strength predicted by using the section analysis of the girder section only or using the strut-and-tie model based on elastic-analysis stress distribution. (2) The ultimate strengths are 22% to 26% larger than the yielding strength. This additional strength derives from the strain hardening of yielded reinforcements and the shear resistance due to continuity with the adjacent span. (3) The pattern of shear force flow and failure mode in shear zone varies depending on the amount of vertical shear reinforcement. And (4) it is necessary to take into account the existence of the upper wall in the analysis and design of the deep continuous transfer girders that support the upper wall with a long end shear span.

Keywords: reinforced concrete; continuous deep girder; strut-and-tie model; DIANA; shear capacity.

1. Introduction

One of the structural systems for multi-purpose buildings in Korea is a combination of a moment-resisting frame for the lower stories and a bearing-wall system for the upper stories. The lower stories usually accommodate parking areas, commercial spaces, gardens, or open spaces for architectural purposes, while the upper stories are generally used for residential apartments. In this type of building structures, transfer girders transmit the load from the upper bearing wall to the lower frame. Girders support walls that are set back from the column lines, and are generally deep. Therefore, the principle of Bernoulli ("A plane section remains a plane after deformation") does not apply. Nevertheless, most of practicing structural engineers still apply this principle to the design of

*Corresponding author, Professor, E-mail: hslee@korea.ac.kr

^aAssistant Professor

^bEngineer

these girders because of nonexistence of any viable alternative. This convention can be uneconomical and causes difficulties in construction due to the excessive depth of the beams and the congested reinforcement. Moreover, the resulting design may not necessarily ensure safety and efficiency in structural behavior. While the procedure of strut-and-tie modeling has recently been introduced as an alternative, this method still needs more experimental verification for practical application with confidence, despite the general recommendation recently proposed in the Appendix of ACI 318-05 (ACI 2005).

Over the past several decades, many researchers have conducted experiments to increase the shear capacity of reinforced concrete deep beams, and have proposed new design methodology for effectively predicting or estimating the capacity and the mode of failure of deep beams (Kong *et al.* 1970, Tan *et al.* 1995, Aguilar *et al.* 2002, Zararis 2003). Since the strut-and-tie procedure for the design of stress-disturbed members or regions (Schlaich *et al.* 1987), many researchers have applied this model to deep beams for developing design methods or equations, and have verified their proposals by comparing them with test results (Saio 1995, Manamoros and Wong 2003, Tang and Tan 2004, Cook and Mitchell 1988). Simplified method was proposed for predicting shear strength and deflection for RC deep beams based on softened strut-and-tie model (Hwang *et al.* 2000, Lu *et al.* 2010). Pimentel, Cachim and Figueiras conducted an experimental and numerical research to gain a deeper insight on the structural behavior of deep girders with indirect support and to assess the size effects in the ultimate state behaviour (2008). Rogowsky, MacGregor and Wong showed that the ductile behavior of continuous deep girders can be ensured by the use of strut-and-tie models (1986). However, the adopted example was a two-span deep girder that transmits the load from the upper columns to the off-set lower columns and whose shear span to depth ratios are 1.5 and 2.0. Recently, Zhang and Tan proposed a direct strut-and-tie model accounting for stress-distribution factors and verified their model with the experimental results (2007), and also suggested a new model which takes into account the effect of the support stiffness in continuous girders lately (2010). Wu and Li (2009) showed that the specimens of continuous deep girders having openings designed according to ACI 318-02 (2002) had larger strengths than expected and that the design was on the safe side. A new model was proposed to predict the effect of shear and web reinforcements around the openings in continuous girders and the efficiency of the model was proved through experiments by comparing with the existing equations (Yang *et al.* 2007, Yang and Ashour 2008). All the researches were addressed to the continuous deep girders which transmit the load from the upper columns to the offset lower columns. This study is concentrated on the continuous deep reinforced concrete girders which support the upper wall rather than columns. In this case, the upper wall can be an acting load as well as an integrant resisting element with the supporting girders.

The objective of this paper is to clarify the behavioral characteristics of the reinforced concrete continuous deep girders, which transmit the gravity load from the upper wall to the lower columns with a long end shear span in which shear-span-to-height ratios range from 1.8 to 2.5. To achieve this objective, a 17-story reinforced concrete structure was selected as a prototype. The continuous transfer girder between the upper wall system and the lower frame was designed in accordance with: (1) the conventional method based on the assumption of beam theory; and (2) the strut-and-tie method. However, it should be noted that the details of the strut-and-tie method applied herein differ from the recommendations in the late versions of ACI 318, which was not available at the time of experiment in 1999. The design procedures and final details were compared, and experiments were conducted to investigate the behavior of specimens. Since the information obtained through

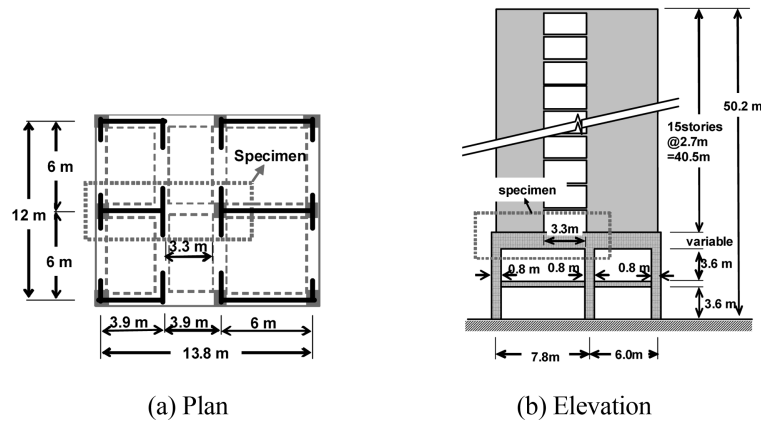


Fig. 1 Prototype building

experiments was limited to a few measured histories of displacements, strains, and forces with the crack and damage distributions, an analytical study was performed using the nonlinear-analysis program DIANA (De Witte and Wolthers 2005) to overcome this limitation and exploit more information from the test results. Two design approaches are evaluated on the basis of these experimental and analytical studies.

2. Design of continuous transfer girders having long end shear spans

Fig. 1 shows the prototype of a multi-purpose building structure. The upper 15 stories are constructed as a bearing-wall structure, and the lower two stories consist of a space frame. The two-span continuous deep girder transmits the gravity load from the upper bearing wall to the lower columns. While the right span supports the wall over the full length of the span, the left span supports the wall only over the left half length of the span with the right half remaining as shear span. The design strength of the concrete and the reinforcement are 30 MPa and 400 MPa, respectively.

2.1 Design by the conventional procedure

The transfer girder was modeled as a continuous beam. The gravity loads from the upper stories are shown in Fig. 2(a). It was assumed for this design that the upper wall acts as a load rather than as a structural member. The concentrated loads represent the load from the orthogonal walls and girders. The transfer girder was analyzed on the assumption that it has a constant flexural rigidity throughout the length and that the supports by the columns are hinges. The shear and flexural moment diagrams are shown in Figs. 2(b) and (c). The member size, flexural reinforcement and the shear reinforcement were designed in accordance with the requirements of ACI 318-95 (ACI 1995). The total depth was determined to be 1800 mm. The detailed information on the flexural and shear reinforcements is given in Table 1 (AS-1). A comparison of the demand and supply in the flexural moment and the shear force is shown in Table 2.

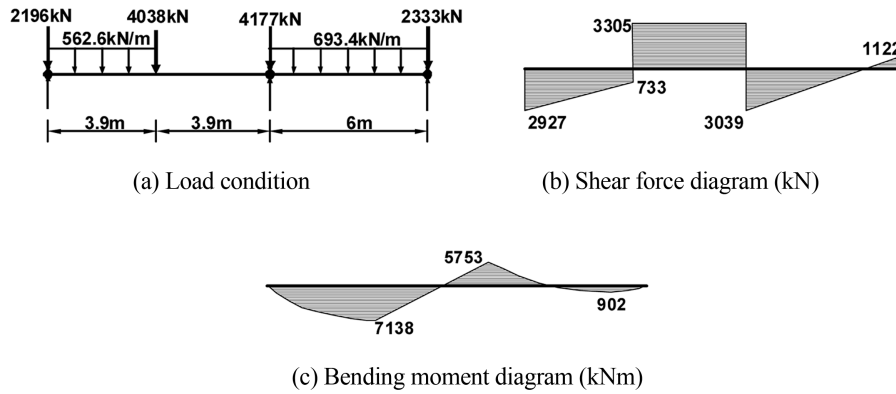


Fig. 2 Load condition and member force diagram for conventional procedure (prototype)

Table 1 Comparison of design results

Shear span (mm)	Design Approach	Width \times height (mm)	Shear span / height ratio (a/h)	Flexural reinforcement		Shear Reinforcement	
				Top bars in support "B"	Bottom bars in mid span	Horizontal (%)	Vertical (%)
3,300	Conventional (AS-1)	800 \times 1,800	1.83	28-D25	34-D25	2-D19@250 (0.2)	4-D13@100 (0.64)
	Strut-and-tie 1 (ST-1)	800 \times 1,800	1.83	24-D25	28-D25	2-D19@250 (0.2)	4-D13@160 (0.40)
	Strut-and-tie 2 (ST-2)	800 \times 1,350	2.44	34-D25	40-D25	2-D19@250 (0.2)	4-D13@100 (0.64)

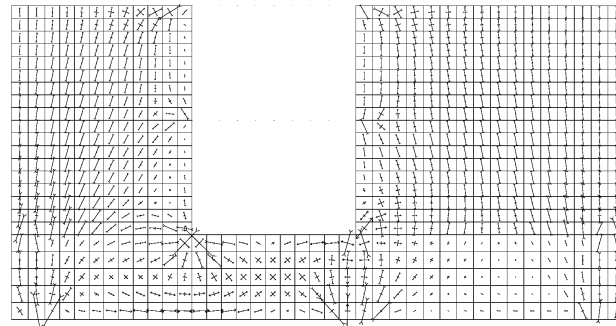
Table 2 Demand and supply member forces

	Member forces	Demand	Supply	Supply/Demand
Conventional (AS-1)	Shear force (kN)	3,305	4,241*	1.28
	Moment (kNm)	7,138	9,670**	1.35
Strut-and-tie 1 (ST-1)	$T_{f-ff} + T_{g-gg} + T_{h-hh}$ (kN)	3,803	4,470	1.18
	T_{dd-ff} (kN)	5,630	5,678	1.01
Strut-and-tie 2 (ST-2)	$T_{f-ff} + T_{g-gg}$ (kN)	3,830	4,606	1.16
	T_{dd-ff} (kN)	8,214	8,212	1.00

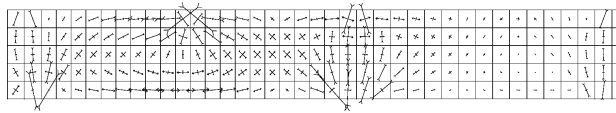
*: ϕV_n , **: ϕM_n .

2.2 Design by the strut-and-tie procedure

The struts and ties are modeled using the guidelines suggested by Schlaich *et al.* (1987) as follows: (1) Elastic finite element analysis is performed to determine the general flow of forces from the upper wall to the transfer girder and finally to the columns. (2) Using this information, the layout of struts and ties are configured. And, (3) this truss model consisting of struts and ties is

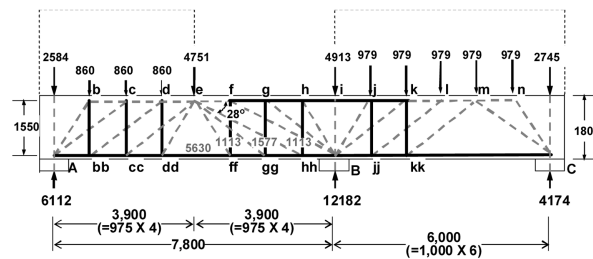


(a) Upper wall + transfer girder

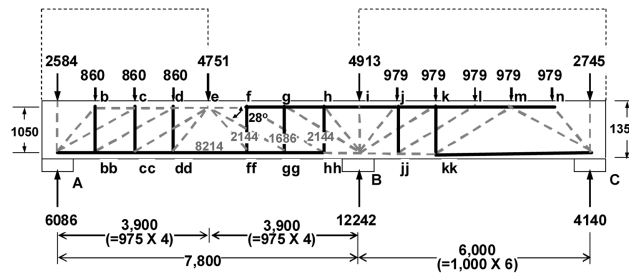


(b) Transfer girder only

Fig. 3 Principal stress distribution by elastic FEA



(a) ST-1



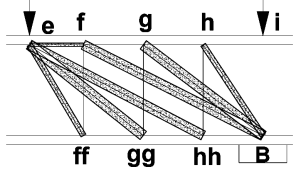
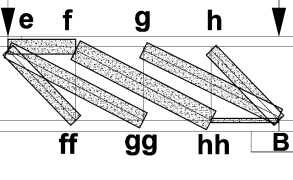
(b) ST-2

Fig. 4 Strut-and-tie models for different-depth girders (prototype) (unit: kN, mm)

analyzed and elements (struts and ties) are checked for the applied forces. Since the distributions of principal stresses in Fig. 3 appear to be similar regardless of the existence of the upper shear wall, the strut-and-tie models were established neglecting the existence of the upper shear wall. The distributed load from the upper wall in Fig. 2(a) was converted to the equivalent concentrated loads at the quarter points which are also designated as nodes in the strut-and-tie model.

All the applied concentrated loads were increased by dividing with the factor of $\phi = 0.85$. The

Table 3 Strut width in the shear region ($f_{ce} = \nu_1 \nu_2 f'_c = (0.8)(0.78)f'_c = 0.625f'_c$)

	Strut	Force (kN)	b (mm)	Width (mm)	Compression strut in the shear region
ST-1	e-f	-844.2	800	56	
	e-ff	-1315.3	800	88	
	e-gg	-2534.9	800	169	
	e-hh	-2377.7	800	159	
	f-B	-2377.7	800	159	
	g-B	-2534.9	800	169	
	h-B	-1315.3	800	88	
ST-2	e-f	-3091.9	800	206	
	e-ff	-2925.5	800	195	
	e-gg	-3556.7	800	237	
	f-hh	-4521.8	800	301	
	g-B	-3556.7	800	237	
	h-B	-2925.5	800	195	
	hh-B	-889.5	800	60	

dimensions of struts were checked by using the effective concrete strength according to MacGregor (1997).

Two strut-and-tie models were developed for two different total depths, $h = 1,800$ mm (ST-1) and $1,350$ mm (ST-2), in Fig. 4. Shear force in the shear span in ST-2 was transmitted at most twice through vertical ties such as the load path e-ff-f-hh-h-B while that in ST-1 was only once. Required and supplied forces of bottom and vertical ties in critical region are compared in Table 2. The struts in the critical shear zone were checked for the availability of the width as shown in Table 3 (MacGregor 1997).

2.3 Comparison of design results

A comparison of the design results obtained from the two approaches is shown in Table 1. Use of strut-and-tie models reduced the vertical shear reinforcement from 0.64% to 0.40% with the same depth of 1800 mm, or the total depth from 1,800 mm to 1,350 mm with the same shear reinforcement of 0.64% when compared with those of the conventional approach. The positive longitudinal reinforcement was reduced from 34-D25 in AS-1 to 28-D25 in ST-1 and increased to 40-D25 in ST-2, while the negative decreased from 28-D25 in AS-1 to 24-D25 in ST-1 and increased to 34-D25 in ST-2.

3. Construction of specimens and experimental setup

The available loading system shown in Fig. 5(b) consists of a strong frame and an actuator acting downward at the top of the frame. Since the smallest diameter of commercially available deformed reinforcements was D5, the largest possible reduction scale was 1:2.5 unless smaller scale

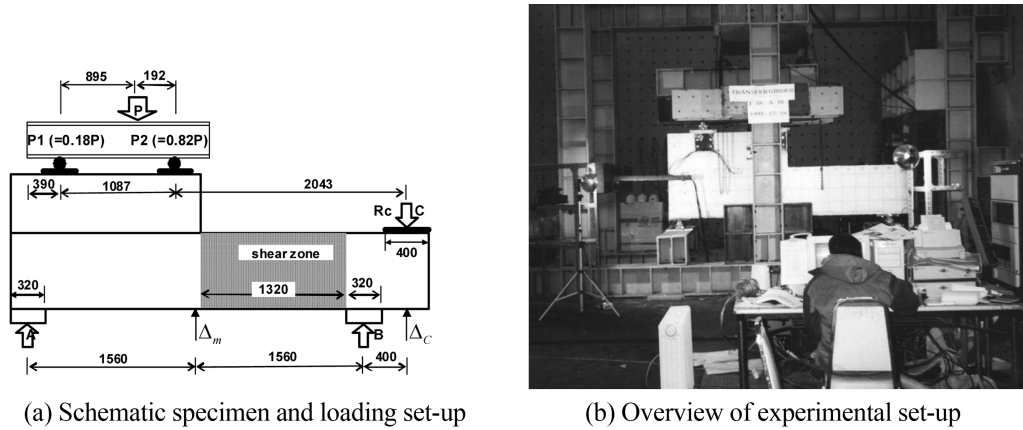


Fig. 5 Loading system and specimen (unit: mm)

reinforcements were to be made on the authors' effort. Furthermore, there were two more constraints imposed by the loading system. Since the length of the whole two-span continuous girder could not be accommodated within the strong frame, the right-hand span of the continuous girder should be truncated and the continuity at support B simulated with the upper-bound passive support at C as shown in Fig. 5(a). And, because only one actuator was available, the number of loading points in the wall region in the left span should be reduced, leading to the two-point simplified loading system in Fig. 5(a). With all these modifications of the prototype to the specimens, it was further found that the range of the load to be applied exceeded the capacity of the available loading system. Therefore, the width of the specimen had to be reduced by half. However, in this case, the width of the upper wall could be too thin to carry the applied concentrated loads without bearing failure over to the transfer girder. Thus, the width of the upper wall was increased by two times. Displacement transducers were installed to measure: the vertical displacement, Δ_m , at the mid-span; and the displacement, Δ_c , at the bottom of the upper-right-hand support, C, where a load cell was inserted to measure the reaction force at top of the specimens. Strain gauges were attached to the reinforcements to measure the strains of the flexural and shear (vertical and horizontal) reinforcements at the critical locations. The overview of the test set-up is given in Fig. 5(b).

Fig. 6 shows the resulting details of three specimens: AS-72 representing the prototype designed through the conventional approach, and SS-72 and SS-54 for the prototypes, ST-1 and ST-2, respectively. The average concrete compressive strengths of AS-72, SS-72, and SS-54 were 35 MPa, 41 MPa, and 43 MPa, respectively, which are larger than the design strength (30 MPa). The main reinforcements of the specimens were D10 bars, while the shear reinforcements were D5 bars, with the average yield strengths being 432 MPa and 461 MPa, respectively.

With modification of loading and boundary conditions, it becomes clear that there should be some changes in the external reactions and internal force distributions originally assumed in the design of the prototypes as given in Fig. 2 and Fig. 4. Strut-and-tie models satisfying the equilibrium conditions with the changed loading and boundary conditions are given for the specimens SS-72 and SS-54 in Fig. 7. Also, the shear force and bending moment distributions with the assumptions of constant flexural rigidity through the length of the beam and the fixed hinge at support C were obtained for the specimen, AS-72. The maximum member forces for the 1: 2.5 scale specimens

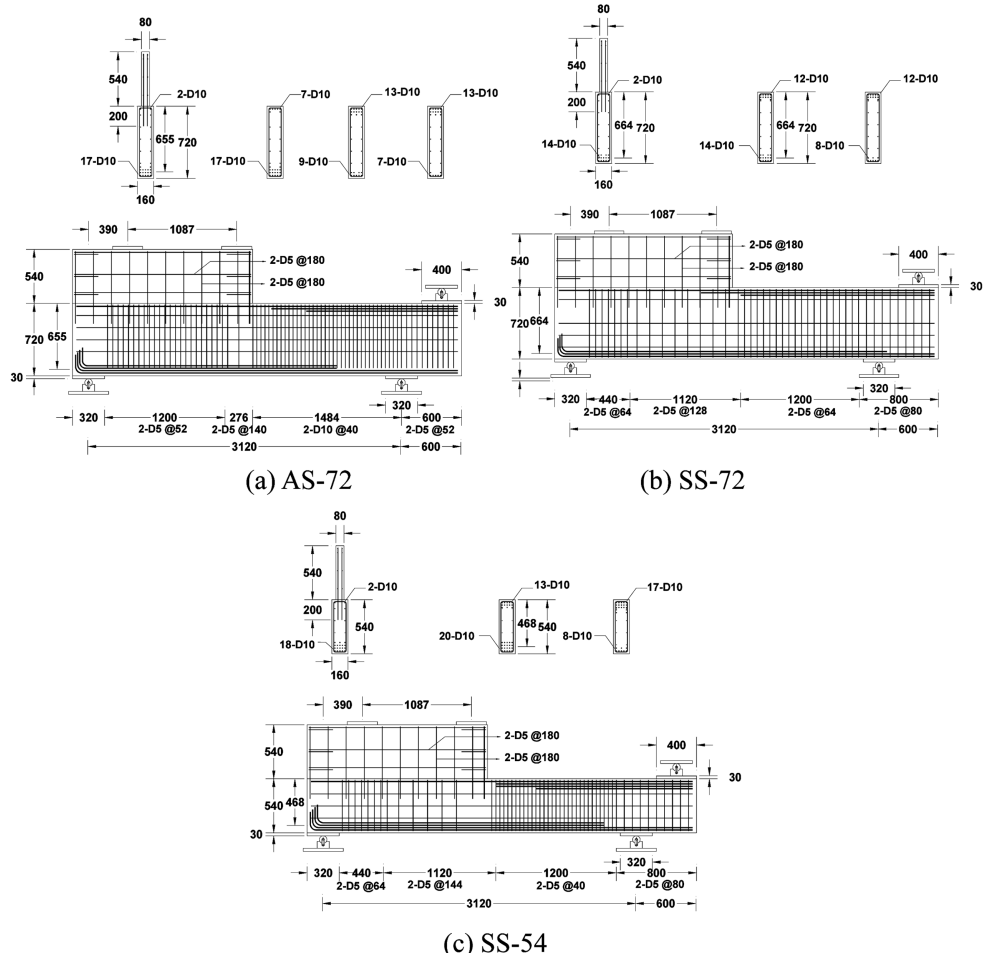


Fig. 6 Details of specimens (scale: 1/2.5, unit: mm)

Table 4 Comparison of member forces for prototype and scaled models under experimental condition

Prototype/Specimen		(1) Prototype	(2) Reduced by similitude	(3) Experimental B.C.*	(4) Experimental Result	(5) (4)/(2)
Conventional (AS-1/AS-72)	P_u (kN)	6,232	498	498	808	1.62
	$V_{u, \max}$ (kN)	3,305	264	276	375	1.42
	$M_{u, \max}^+$ (kNm)	7,138	228	230	484	2.12
Strut-and-tie 1 (ST-1/SS-72)	P_u/ϕ (kN)	7,332	586	586	706	1.20
	$V_{u, \max}$ (kN)	3,803	304	280	315	1.04
	$M_{u, \max}^+$ (kNm)	8,728	279	337	443	1.59
Strut-and-tie 2 (ST-2/SS-54)	P_u/ϕ (kN)	7,332	586	586	638	1.09
	$V_{u, \max}$ (kN)	3,830	306	291	298	0.97
	$M_{u, \max}^+$ (kNm)	8,627	276	319	379	1.37

*: For the boundary condition, see Fig. 7 and Fig. 8.

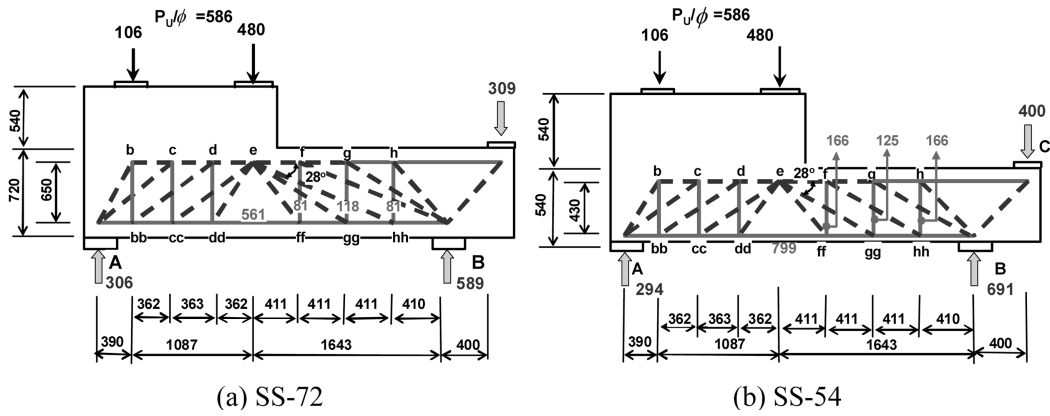


Fig. 7 Strut-and-tie model for experimental boundary condition (unit: kN, mm)

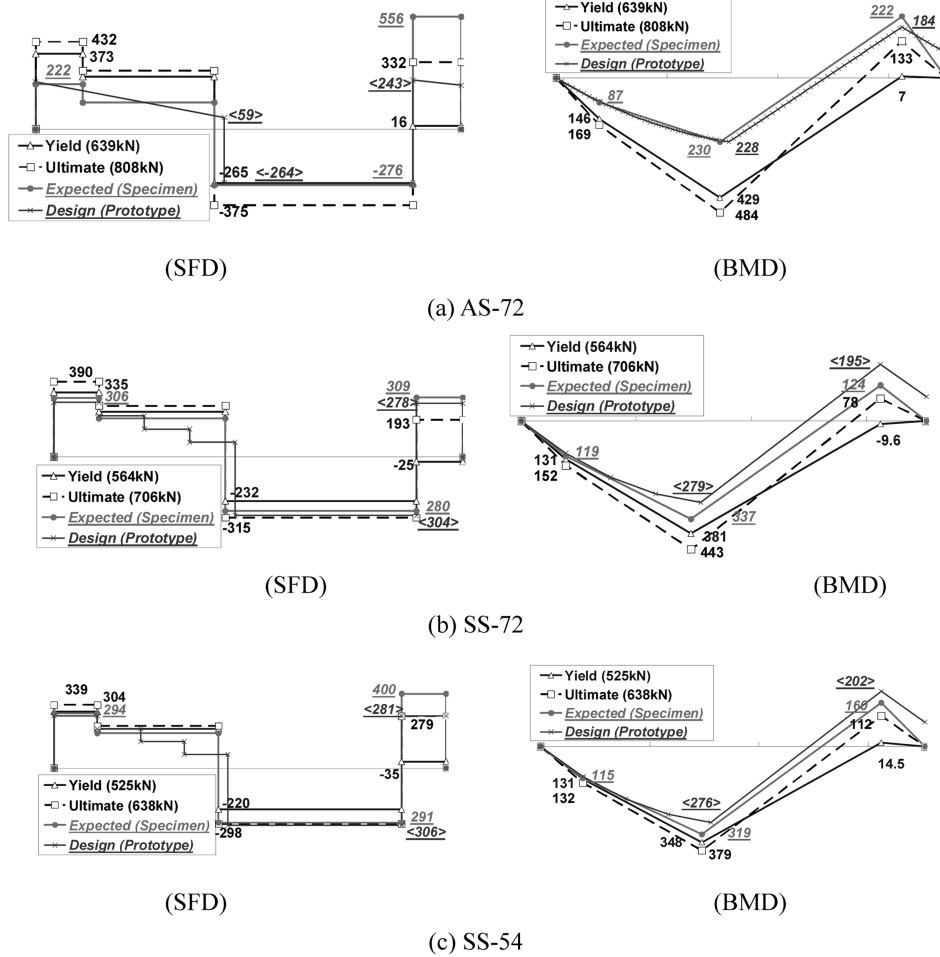


Fig. 8 Comparison of member forces between design and experiment

derived according to the similitude from the prototypes and those estimated through the above procedures are compared in Table 4 while the distributions of shear force and bending moment are compared between the design in prototype (blue line) and the expected by the changed conditions in experiment (red line) in Fig. 8. It can be found that these two distributions are very similar though some minor differences exist in the bending moment diagrams. The diagrams corresponding to yield and ultimate strength obtained from experiment are overlapped in this figure and will be discussed later.

4. Test results

4.1 Global behavior

Fig. 9(a) shows the relationship between the applied total load, P , and the vertical displacement, Δ_m , at mid-span with solid lines. The ultimate strengths appear to be 1.28~1.62 times larger than the design strength, P_u . The global responses of three specimens are summarized in Table 5. In this table, the measured values of yield bending moments, $M_{y,measured}$, are larger than those of the girder sections, obtained through using the first principles of section analysis for girder only, M_{y1} , but lower than those of the sections including the upper wall, M_{y2} . This indicates that it is inappropriate to apply the beam theory to this type of transfer girders and that the strut-and-tie model should include some portion of the upper wall even though the principal stress distributions by linear elastic finite element analyses do not make much difference with and without upper wall as shown in Fig. 3.

All the values of deflection under the service load $P_{(D+L)} = 342$ kN in column (5) of Table 5 are within the limit of 1/480. Though the ductility ratio of δ_u/δ_y in column (7) varies from 2.45 for SS-54 to 4.32 for AS-72, deformability in column (6) appears to be similar.

The relationships between the shear force in the shaded shear region and the flexural moment at the load point, P2, in Fig. 5(a), are given in Fig. 9(b), where it can be found that (1) the curves up to the flexural yielding keep the linearity between the shear and moment, but (2) after this yielding the shear forces only keep increasing with the moments remaining approximately constant. The finding that the reaction at support C started to occur approximately at the time of flexural yielding

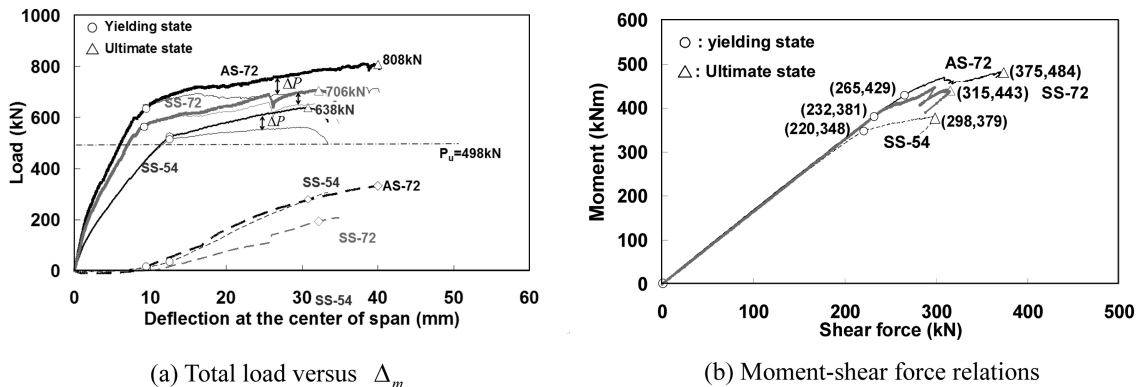


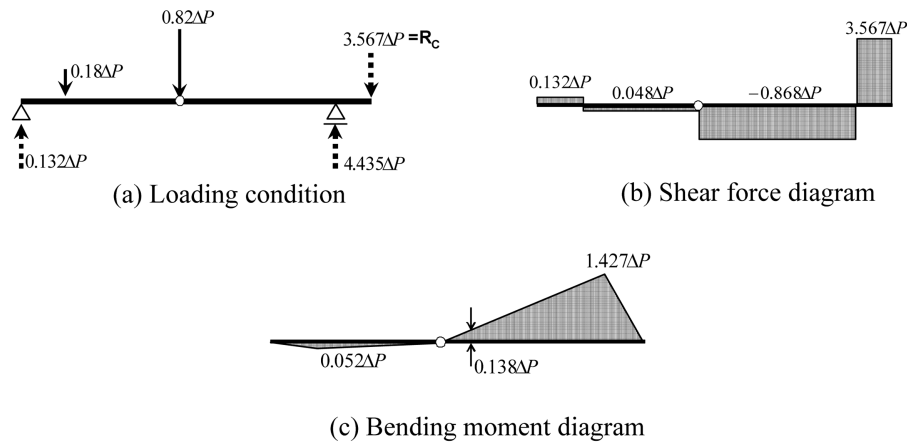
Fig. 9 Global behavior of specimens

Table 5 Summary of experimental results (Ultimate strength and ductility)

Specimen	(1) P_{\max}/P_y (kN)	(2) V_{\max}/V_y (kN)	(3) $\Delta P/P_{\max}$	(4) M_y (kNm) $M_{y, \text{means}}/M_{y1}^*/M_{y2}^{**}$	(5) Δ/l (D+L) (mm/mm)	(6) δ_u (mm)	(7) μ_Δ
AS-72	1.26 (=808/639)	1.42 (=379/265)	0.12 (=93/808)	429 / 293 / 546	3.34/3120 (=0.51/480)	40.81	4.32
SS-72	1.25 (=706/564)	1.36 (=315/232)	0.08 (=54/706)	381 / 255 / 532	4.0/3120 (=0.62/480)	31.81	3.47
SS-54	1.22 (=638/525)	1.35 (=298/220)	0.12 (=78/638)	348 / 242 / 584	6.83/3120 (=1.05/480)	30.76	2.45

*Calculated moment capacity of girder only

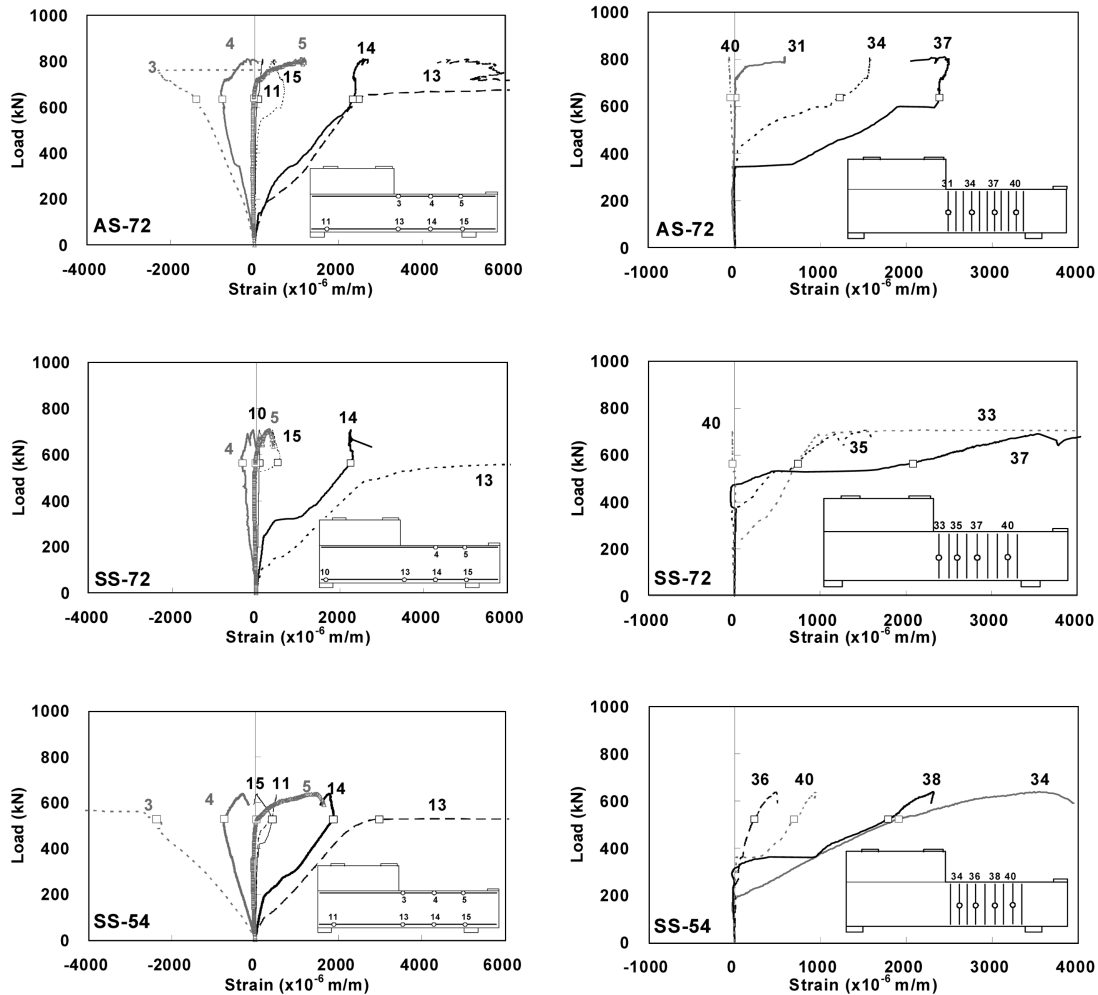
**Calculated moment capacity of girder including wall

Fig. 10 Load condition, SFD, and BMD in equilibrium with ΔP and R_c with a hinge at point P2

at the load point P2 in Fig. 5(a) enables the specimens to be modeled as a continuous beam with a hinge located at the load point P2 as shown in Fig. 10(a), where the reaction force, R_c , is in equilibrium with the additional load, ΔP . With this model, the incremental shear force, ΔV , and the incremental flexural moment, ΔM , can be calculated with the relation of $R_c = 3.567\Delta P$. Using measured values of R_c , the curve of $P - \Delta P$ versus mid-span deflection is given with weaker solid lines in Fig. 9(a). The values of ΔP at ultimate strength are given in column 3 of Table 5 and it is interesting to note that the value of $\Delta P/P_{\max}$ in SS-72 is smaller than that in SS-54 even though the depth of SS-72 is 33% larger than that of SS-54.

4.2 Distribution of strains in reinforcement

Fig. 11 shows the distribution of strains in longitudinal and vertical shear reinforcement for the specimens. For all the specimens, the strains at location 13 of the bottom longitudinal reinforcement show the yield plateau at yield strength and keep increasing up to the ultimate strength while the strains at location 14 remain almost constant after reaching some values at yielding of location 13.



(a) Distribution of strain in longitudinal reinforcements (b) Distribution of strain in vertical shear reinforcements

Fig. 11 Distribution of strains in reinforcement

This phenomenon implies the concentration of yielding to a confined region of the reinforcement. Amounts of strains at locations, 10, 11, and 15, appear to be negligible up to the ultimate strength. Therefore, the requirements for anchorage may be alleviated in the end regions. The strains at locations, 4 and 5, of the top longitudinal reinforcement were increasing in compression at the beginning, but, above the yield strength, changed the direction from compression to tension though the absolute values of strain remained relatively small. The strains at location 3 were always increasing in compression and reached (AS-72) or exceeded (SS-54) the yield strain above the yield strength.

AS-72 did not show any significant yielding in vertical shear reinforcements and the strains at locations, 34 and 37, remained almost constant above the yielding load. This means that the resisting mechanism in shear zone, as shown in Fig. 14, is through the two distinct struts passing

across these vertical bars. SS-72 revealed significant yielding at location 37, where a major diagonal crack occurred as shown in Fig. 12. However, while the strain at location 35 started to occur above $P = 380$ kN and increased up to the ultimate strength without yielding, the strain at location 33 started much earlier at about $P = 200$ kN, kept increasing, and finally reached the yield plateau at the ultimate load. SS-54 experienced relatively early initiation of strain development in the vertical reinforcements all over the girder. While all the vertical bars did not yield at the yielding load, $P_y = 525$ kN, strains at locations, 34 and 38, had just reached or exceeded the yield point at the ultimate strength.

4.3 Failure modes

Fig. 12(a) shows crack distributions for three specimens just before the final failure through the concrete crushing or uplift in the highly compressed regions in Fig. 12(b). After specimen AS-72

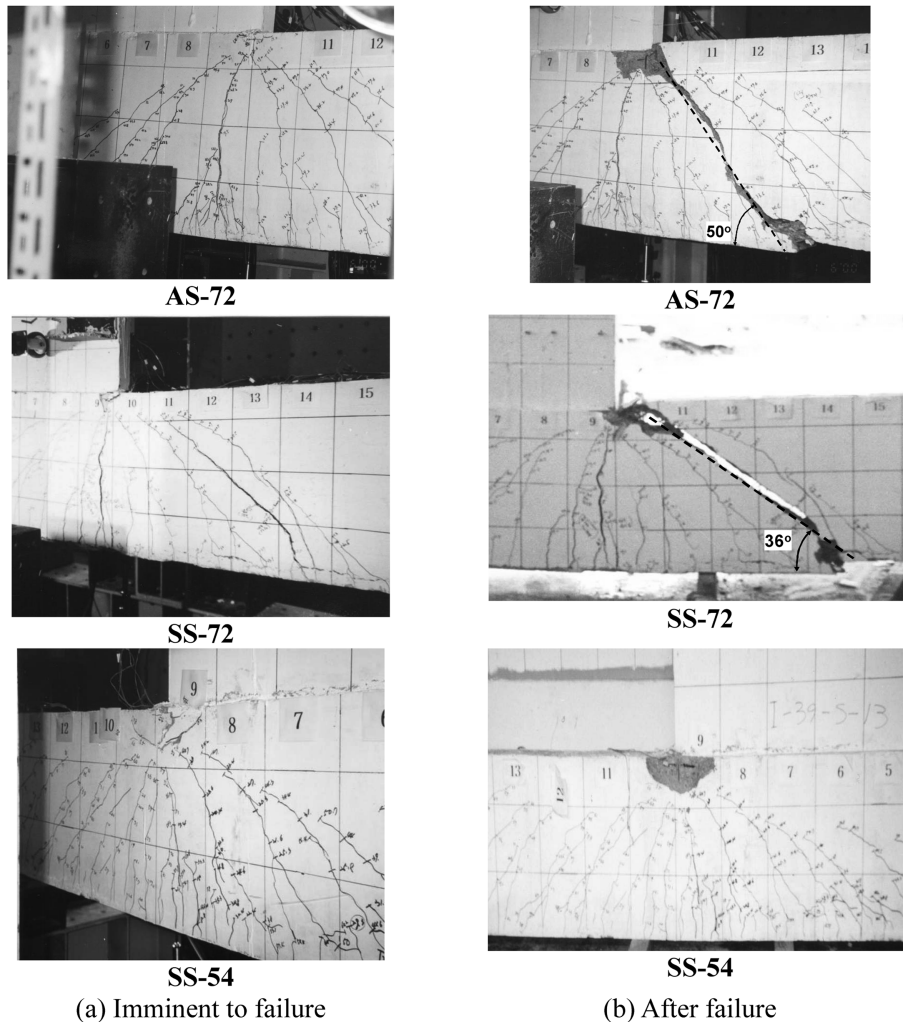


Fig. 12 Crack distribution and failure mode

underwent flexural yielding approximately at $P = 600$ kN, the vertical crack under the loading point P2 among many cracks kept widening. The ductile behavior after the flexural yield induced a number of more cracks in shear and flexural regions. The sudden concrete compression crushing in the top corner portion of girder just beneath the wall led to the total collapse accompanied by the shear failure through a diagonal shear crack and the fracture of the vertical reinforcements.

In case of SS-72, vertical flexural cracks started to occur around the mid-span at the load $P = 190$ kN. The number of diagonal cracks increased as the load increased up to $P = 540$ kN. Above this load, the width of a major diagonal crack only revealed significant increase. This diagonal crack had eventually penetrated the whole section following the crushing or uplift failure in the upper left compression zone of concrete. The ensuing large widening of the diagonal crack caused fracture of vertical shear reinforcements.

Specimen SS-54 showed a development of many flexural and shear cracks all over the girder up to $P = 600$ kN, above which the compressive crushing of concrete occurred at the reentrant corner of the wall and girder, leading to the sudden loss of resistance. The failure mode of this specimen is a typical flexural failure by compressive concrete crushing after yielding of the bottom longitudinal reinforcements whereas other specimens failed in diagonal shear modes.

5. Analytical simulation of the test results

5.1 Analytical modeling and correlation with experimental results

The objective of the analytical simulation of test results is twofold: (1) to obtain the unknown information on the test results such as the effects of support rigidities and internal force distributions, and (2) to check the reliability of the currently available nonlinear analysis software in prediction of nonlinear behavior of concrete structures. For these objectives, a nonlinear finite element analysis program, DIANA (De Witte and Kikstra 2005), was used. The material model of Drucker-Prager yield criteria with tension cut-off model for concrete with the values of parameters in Table 6 and the elastic-plastic stress-strain relationship for D5 and D10 reinforcements were adopted. Supports, A, B, and C, were modeled using the linear springs with stepped functions of stiffness, which were adjusted arbitrarily to best simulate the test results. More detailed information on the modeling and analysis is directed to reference (Sun 2007).

The final $P-\Delta_m$, $R_c-\Delta_m$, and $P-\Delta_C$ curves and the curves of shear force versus flexural moment obtained through analyses are compared with those of experiment in Fig. 13. The correlations are satisfactory.

Table 6 Material parameters for analysis of specimens

Specimen	f'_c (MPa)	Drucker-Prager parameter	
		ϕ (Deg.)	C (MPa)
AS-72	35	10	14.60
SS-72	41	10	17.12
SS-54	43	10	17.87

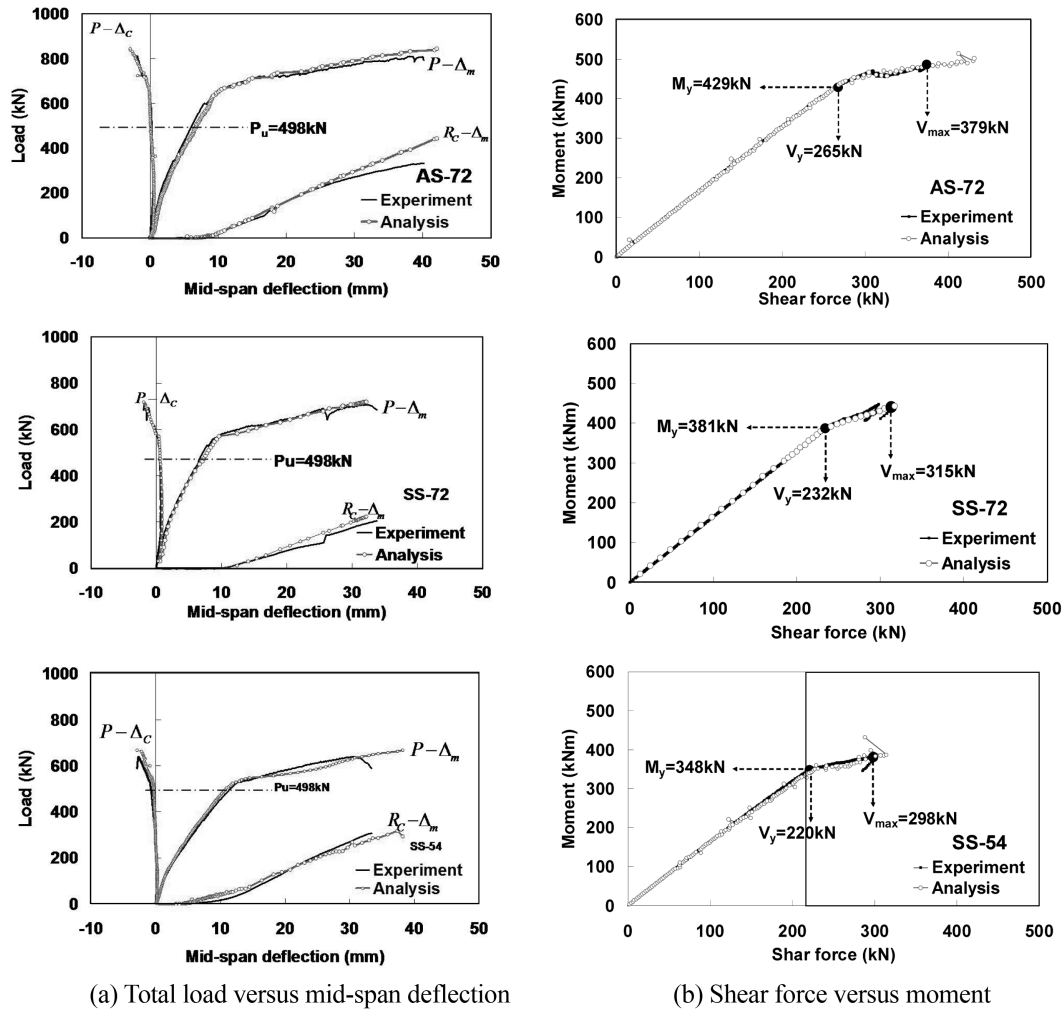


Fig. 13 Correlation between experiment and analysis

5.2 Investigation of internal force flows

Though the failure mode by concrete crushing in experiment could not be simulated due to the limitation of the used Drucker-Prager model, Figs. 14(a) and (b) show clearly the internal force flows in the girders, particularly in the shear regions, through the distributions of von Mises stress at the yield states and the ultimate collapse states in the experiment for three specimens, respectively. It is interesting to note the followings: (1) the patterns of force flow in the shear zone already appear to be different from each other at the yield state and remain almost fixed up to the collapse state; (2) AS-72 shows two distinct diagonal struts with the slope of approximately 50 degree in the shear zone whereas SS-72 reveals only one distinct strut with a slope of about 36 degree. The different slopes cause the difference in the amount of reaction force at support C, between AS-72 and SS-72, as can be noticed in Figs. 9(a); (3) The slope of diagonal strut in the compression field as given in the strut-and-tie model for the design of prototype, ST-1, in Fig. 4(b)

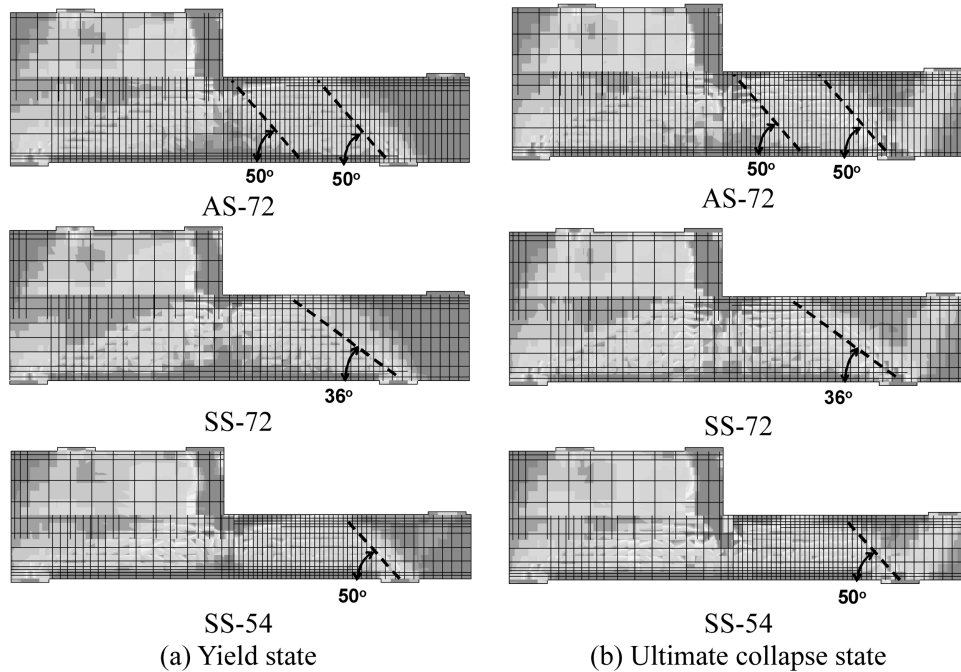


Fig. 14 Distributions of von Mises stress

(represented by the specimen SS-72) is about 28 degree, which is in good agreement with both the slope, 36 degree, of the main diagonal crack in experiment in Fig. 12 and that of force flow in analysis in Fig. 14. It indicates that the strut-and-tie model has excellent potential to predict the capacity of this type of transfer girders; (4) the force flow in the shear zone for SS-54 does not show any distinct strut or struts, but all the region participates in the transmission of the shear force. However, the slope of initiating and terminating struts in the shear zone appears to be about 50 degree, therefore, the amount of reaction at support C, R_C , is similar to that of AS-72 as can be seen in Fig. 9(a). Fig. 12 shows that the flexural and diagonal shear cracks are well dispersed without any concentration of widening on a specific crack, all directing to the reentrant corner region beneath the wall, where the stress concentration occurred and eventually led to the failure by the concrete compressive crushing.

6. Evaluation of design approaches

The strength of the system including the transfer girder and the upper wall together at yielding of the bottom longitudinal reinforcements turns out to be much higher than the strength of the girder itself estimated by using the beam section analysis as shown in Fig. 8. This yield strength already amounts to 105% to 128% of the required strength without any contribution from the top negative reinforcements.

After yielding of the bottom longitudinal bars, the additional load is resisted by the shear transfer through the shear zone and the negative moment to the continuous support C. The concept of compression fan and compression field proposed by MacGregor (1997) can be applied in this case.

The pattern of force flow in the shear zone varies depending on the amount of vertical reinforcement even at the yield stage of the bottom bars. The larger ratio of 0.64% in AS-72 caused two distinct approximately 50-degree concrete struts in the shear zone, whereas the lower ratio of 0.40% in SS-72 had only one distinct strut with the slope of approximately 36 degree even though the original strut-and-tie model used for design contains upper and lower parallel struts with the slope of 28 degree. The results of experiment and analysis for SS-72 reveal that the actual flow of force is through the top horizontal strut (e-f) and then through the upper diagonal strut (f-B) in Fig. 4(a), which is different from the design assumption in the original strut-and-tie model.

The additional or incremental shear after yielding of the bottom bars was transmitted proportionally to the sine of the slope angle of struts in shear zone. Therefore, SS-72 had lower incremental shear than AS-72 in Fig. 9(a). The ultimate strengths of the system including the transfer girder and upper wall were 808 kN, 706 kN, and 638 kN, for AS-72, SS-72, and SS-54, respectively, much larger than the required strength, $P_u = 498$ kN, or $P_u/\phi = 585$ kN. This over-strength is considered to originate mainly from the participation of the upper wall in resistance with the inherent over-strength in yield strength and the strain hardening effect of reinforcements, and to some minor amount from the resistance through the continuity with the adjacent span.

In both of the conventional and strut-and-tie approaches, the final designs contained heavy top reinforcements for the negative moments at support C. However, these heavy reinforcements turn out to be almost useless and can be reduced greatly because (1) the positive yield strength of the system proves to be much higher than the values estimated by using both approaches as shown in Fig. 8 and in the last column of Table 4, and (2) the additional strength up to the ultimate state generally is controlled by the shear capacity of shear zone as can be found in Fig. 8.

The negligence of the contribution of the upper wall is the reason for the erroneous estimation of yield strength in case of the conventional approach, while the use of linear elastic finite element analysis can lead to inappropriate development of the design model in case of the strut-and-tie approach.

7. Conclusions

The design of continuous deep girders transmitting the gravity load from the upper shear wall to the lower columns has always been a challenging task to practicing structural engineers since it is known that the beam theory cannot be applied to this case, while the alternative design approach such as the strut-and-tie method has not been fully elaborated as yet through experimental and analytical verification for practical application with confidence. The study stated herein is aimed at providing useful information to develop a reasonable design approach for continuous reinforced concrete deep girders transmitting the load from the upper wall to the lower columns with long end shear spans.

After a prototype building was selected, design was conducted: (1) by assuming the transfer girder is a continuous beam with a constant size of section and applying all the requirements of ACI 318, (This is called a conventional design approach in this paper.) and (2) by using the strut-and-tie model approach. However, the model was implemented in a different way as recommended in the currently available appendix of ACI 318-05.

Based on the experimental and analytical studies, the following conclusions are drawn:

- (1) The yielding strength of the continuous RC deep girders already amounts to 105% to 128% of

the required strength and is controlled by the tensile yielding strength of the bottom longitudinal reinforcements, being much larger than the nominal strength predicted by using the section analysis when the transfer girder is modeled as beam element, or by using the strut-and-tie model based on elastic-analysis stress distribution. (2) The ultimate strengths are 22 to 26% larger than the yielding strength. This additional strength derives from the strain hardening of yielded reinforcements and the shear resistance due to continuity with the adjacent span. The ultimate strength is governed by the shear capacity of the critical shear zone. (3) The pattern of shear force flow and failure mode in shear zone varied depending on the amount of vertical shear reinforcement. The lower ratio of vertical shear reinforcement induced the flatter diagonal strut and crack failure. With the shear span to total height ratio of 2.5, the failure was governed by flexural behavior. And, (4) it is necessary to take into account the existence of the upper wall in the analysis and design of the deep continuous transfer girders that support the upper wall with a long end shear span.

Acknowledgements

The experimental component of this research was supported during 1998-2000 by the Ministry of Construction and Transportation of the Republic of Korea, the Korea National Housing Corp., as well as by several private companies, including Ssangyong Engineering & Construction Co. Ltd., Kolon Engineering & Construction Co. Ltd., and Hyungsang Structural Engineering Co. Ltd. The analytical component of this research was supported by the Construction Technology Research Center for Tall Buildings, which in turn was sponsored by the Ministry of Construction and Transportation, The Republic of Korea, during 2004-2008.

References

- ACI (1995), *Building Code Requirements for Structural Concrete (ACI 318-95)*, American Concrete Institute, MI.
- ACI (2002), *Building Code Requirements for Structural Concrete (ACI 318-02)*, American Concrete Institute, MI.
- ACI (2005), *Building Code Requirements for Structural Concrete (ACI 318-05)*, American Concrete Institute, MI.
- Aguilar, G., Matamoros, A.B., Parra-Montesinos, G.J., Ramirez, J.A. and Wight, J.K. (2002), "Experimental evaluation of design procedures for shear strength of deep reinforced concrete beams", *ACI Struct. J.*, **99**(4), 539-548.
- Cook, W.D. and Mitchell, D. (1988), "Studies of disturbed regions near discontinuities in reinforced concrete members", *ACI Struct. J.*, **85**(2), 206-216.
- De Witte, F.C. and Kikstra, W.P. (2005), *DIANA – Finite Element Analysis*, TNO DIANA BV.
- Hwang, S.J., Lu, W.Y. and Lee, H.J. (2000), "Shear strength prediction for deep beams", *ACI Struct. J.*, **97**(3), 367-376.
- Kong, F.K., Robins, P.J. and Short, D.R. (1970), "Deep beams with inclined web reinforcement", *ACI J.*, **69**(6), 172-176.
- Lu, W.Y., Hwang, S.J. and Lin, I.J. (2010), "Deflection prediction for reinforced concrete deep beams", *Comput. Concrete*, **7**(1), 1-16.
- MacGregor, J.G. (1997), *Reinforced Concrete Mechanics and Design*, Prentice Hall.
- Manamoros, A.B. and Wong, K.H. (2003), "Design of simply supported deep beams using strut-and-tie models", *ACI Struct. J.*, **100**(6), 704-712.

- Pimentel, M., Cachim, P. and Figueiras, J. (2008), "Deep-beams with indirect supports: numerical modelling and experimental assessment", *Comput. Concrete*, **5**(2), 117-134.
- Rogowsky, D.M., MacGregor, J.G. and Ong, S.Y. (1986), "Tests of Reinforced Concrete Deep Beams", *ACI Struct. J.*, **83**(4), 614-623.
- Schlaich, J., Schafer, K. and Jennewein, M. (1987), "Toward a consistent design of structural concrete", *PCI J.*, **32**, 74-150.
- Siao, W.B. (1995), "Deep beams revisited", *ACI Struct. J.*, **92**(1), 95-102.
- Sun, S.M. (2007), "Analytical Study on the Nonlinear Behavior of RC Transfer Girder", Master Thesis of Korea University. (in Korean)
- Tan, K.H., Teng, S., Guan, L.W. and Kong, F.K. (1995), "High strength concrete deep beams with effective span and shear span variations", *ACI Struct. J.*, **92**(4), 395-405.
- Tang, C.Y. and Tan, K.H. (2004), "Interactive mechanical models for shear strength of deep beams", *J. Struct. Eng.-ASCE*, **130**(10), 1534-1544.
- Wu, T. and Li, B. (2009), "Experimental verification of continuous deep beams with openings designed using strut-and-tie modeling", *IES J. Part A, Civil Struct. Eng.*, **2**(4), 282-295.
- Yang, K.H. and Ashour, A.F. (2008), "Effectiveness of web reinforcement around openings in continuous concrete deep beams", *ACI Struct. J.*, **105**(4), 414-424.
- Yang, K.H., Chung, H.S. and Ashour, A.F. (2007), "Influence of shear reinforcement on reinforced concrete continuous deep beams", *ACI Struct. J.*, **104**(4), 420-429.
- Zararis, D. (2003), "Shear compression failure in reinforced concrete deep beams", *J. Struct. Eng.-ASCE*, **129**(4), 544-553.
- Zhang, N. and Tan, K.H. (2007), "Direct strut-and-tie model for single span and continuous deep beams", *Eng. Struct.*, **29**(12), 2987-3001.
- Zhang, N. and Tan, K.H. (2010), "Effect of support settlement on continuous deep beams and STM modeling", *Eng. Struct.*, **32**(2), 361-372.